Exploiting the MUC5AC Antigen for Noninvasive Identification of Pancreatic Cancer

Kelly E. Henry[*1], Travis M. Shaffer[*1,2], Kyeara N. Mack[1,3], Janine Ring[1], Anuja Ogirala[1], Susanne Klein-Scory[4], Christina Eilert-Micus[4], Wolff Schmiegel[4], Thilo Bracht[5], Barbara Sitek[5], Marguerite Clyne[6], Colm J. Reid[6], Bence Sipos[7], Jason S. Lewis[1,3,8,9], Holger Kalthoff[10], and Jan Grimm[1,3,8]

[1]Department of Radiology, Memorial Sloan Kettering Cancer Center, New York, New York; [2]Department of Radiology, Stanford University, Stanford, California; [3]Molecular Pharmacology Program, Memorial Sloan Kettering Cancer Center, New York, New York; [4]Department of Medicine, Ruhr University Bochum, Bochum, Germany; [5]Medical Proteome Center, Ruhr University Bochum, Bochum, Germany; [6]School of Medicine, Health Sciences Centre, University College Dublin, Dublin, Ireland; [7]Department of Medical Oncology and Pneumology, University Hospital Tübingen, Tübingen, Germany; [8]Departments of Pharmacology and Radiology, Weill Cornell Medical College, New York, New York; [9]Radiochemistry and Molecular Imaging Probes Core, Memorial Sloan Kettering Cancer Center, New York, New York; and [10]Institute for Experimental Cancer Research, Christian-Albrechts University, Kiel, Germany

Pancreatic cancer (PC) remains the fourth leading cause of cancer death; therefore, there is a clinically unmet need for novel therapeutics and diagnostic markers to treat this devastating disease. Physicians often rely on biopsy or CT for diagnosis, but more specific protein biomarkers are highly desired to assess the stage and severity of PC in a noninvasive manner. Serum biomarkers such as carbohydrate antigen 19-9 are of particular interest as they are commonly elevated in PC but have exhibited suboptimal performance in the clinic. MUC5AC has emerged as a useful serum biomarker that is specific for PC versus inflammation. We developed RA96, an anti-MUC5AC antibody, to gauge its utility in PC diagnosis through immunohistochemical analysis and whole-body PET in PC. **Methods:** In this study, extensive biochemical characterization determined MUC5AC as the antigen for RA96. We then determined the utility of RA96 for MUC5AC immunohistochemistry on clinical PC and preclinical PC. Finally, we radiolabeled RA96 with ^{89}Zr to assess its application as a whole-body PET radiotracer for MUC5AC quantification in PC. **Results:** Immunohistochemical staining with RA96 distinguished chronic pancreatitis, pancreatic intraepithelial neoplasia, and varying grades of pancreatic ductal adenocarcinoma in clinical samples. ^{89}Zr-desferrioxamine-RA96 was able to detect MUC5AC with high specificity in mice bearing capan-2 xenografts. **Conclusion:** Our study demonstrated that RA96 can differentiate between inflammation and PC, improving the fidelity of PC diagnosis. Our immuno-PET tracer ^{89}Zr-desferrioxamine-RA96 shows specific detection of MUC5AC-positive tumors in vivo, highlighting the utility of MUC5AC targeting for diagnosis of PC.

Key Words: pancreatic cancer; RA96; immuno-PET; 89Zr; MUC5AC

J Nucl Med 2021; 62:1384–1390
DOI: 10.2967/jnumed.120.256776

Pancreatic cancer (PC) is a devastating disease with a 5-y survival rate of only 9% (*1*). Poor survival for PC patients is most often associated with a late-stage diagnosis, when the disease has already spread and continues to exhibit rapid metastatic progression. PC has few reliable biomarkers that are able to properly diagnose and guide treatment, especially within the window of early detection. As PC is inevitably more difficult to treat at this stage, biomarkers that can diagnose PC in asymptomatic patients may allow more patients to undergo potential curative tumor resection and greatly improve their prognosis.

Serum biomarkers as an indicator for disease are incredibly useful and can be tested routinely from blood work in patients (*2*). Elevated levels of carbohydrate antigen 19-9 (CA19-9) in the blood of patients with PC are typically a red flag in the clinical follow-up (*3*). If CA19-9 levels are abnormal, recurrence has to be assumed and patients are guided to have additional work-up, including abdominal CT scans or MRI (*4*). However, CA19-9 is elevated in approximately only 65% of PC, is not always elevated early in the disease, and can also be elevated in nonmalignant conditions such as chronic pancreatitis (CP) and other inflammatory disorders (*2*). As such, CA19-9 remains suboptimal for PC detection.

Recent evidence has shown that other serum biomarkers, such as mucins, may be more specific and detectable, particularly for differentiating inflammation from oncogenic lesions (*5,6*). Comprehensive genomic analyses of normal pancreas versus CP and PC tissue identified MUC5AC as the most differentially expressed mucin gene compared with benign pancreatic pathologies (*5,7,8*). MUC5AC belongs to a group of high-molecular-weight *O*-glycoproteins that are either secreted or membrane-bound (*5*). MUC5AC was further validated as a useful biomarker both in tandem with CA19-9 and independently when it comes to PC diagnosis (*8–10*) but has never been targeted for imaging.

In this study, we developed an antibody against MUC5AC and applied it for both immunohistochemical analysis and immuno-PET for PC diagnosis. Uptake of radiolabeled MUC5AC showed successful tumor delineation in a PC xenograft out to 144 h after injection of the radiotracer. The uptake of our radiotracer in vivo was blockable, as was demonstrated by a coinjection of excess unlabeled antibody, and also was significantly increased compared with the IgG control ($P < 0.001$), marking its specificity for the

Received Sep. 11, 2020; revision accepted Jan. 13, 2021.
For correspondence or reprints, contact Jan Grimm (grimmj@mskcc.org).
*Contributed equally to this work.
Published online March 12, 2021.

MUC5AC target. We postulate that our anti-MUC5AC antibody has the potential to improve diagnosis of PC both in vivo and ex vivo and change the paradigm for PC serum biomarkers.

MATERIALS AND METHODS

Cell Culture

All tissue culturing was performed using sterile techniques, and all cells were grown at 37°C and 5% CO_2 in a humidified atmosphere according to ATCC instructions. All cell lines discussed in this article were thawed from the same original stocks and routinely tested for *Mycoplasma* contamination.

RA96 Antibody, Protein Extraction, and RA96 Antigen Preparation

RA96 antibody was developed against intra- and intercellular tumor-associated antigens. Secretomes were obtained from supernatants of cells cultured for 48 h in serum-free media and prepared as previously described by us (*11*). Aliquots of lysates (50 μg) or aliquots of secretomes (15 μg) were separated in horizontal 1% agarose gels less than 5 mm thick (high-electroendosmosis, ultra-quality; CarlRoth) with running buffer (40 mM Tris-acetate, 1 mM ethylenediaminetetraacetic acid, and 0.1% sodium dodecyl sulfate, pH 8.0) according to previously published procedures (*12*).

Immunoprecipitation

As antigen sources, the secretomes (40 μg) or the lysates (200 μg) from RA96-reactive and nonreactive cells were used for immunoprecipitation. For comparative analyses, an alternative antibody against MUC5AC—2-11M1—was used in parallel to the RA96 hybridoma supernatant. The antibody 2-11M1 detects the globular D1/D2 domain located in the N terminus of MUC5AC (*13*).

Mass Spectrometry (MS) and Data Mining

Gel pieces containing the antibody-reactive or corresponding nonreactive signals were excised from the nonblotted gel part corresponding to the RA96-reactive region and subjected to the tryptic digestion procedure. The peptides were analyzed by liquid chromatography–tandem MS on a Q Exactive HF instrument (Thermo Fisher Scientific) coupled to an Ultimate 3000 RSLCnano high-performance liquid chromatography system (Dionex) as described previously (*14*). The lists of identified proteins from positive and corresponding negative samples were compared, and accession numbers found exclusively in positive control gel pieces were defined (Supplemental Table 1). A compilation of annotated tandem MS spectra can be found in the supplemental materials. Further criteria for the antigen identification were that the putative RA96 antigen had to be a high-molecular-mass protein of more than 300 kDa and could be associated with or belong to the mucin family (*15*).

Knockdown of MUC5AC and Recombinant Expression of MUC5AC Fragments

To further demonstrate that MUC5AC is the antigen for RA96 antibody, we performed small interfering RNA (siRNA) knockdown experiments and expression experiments on recombinant MUC5AC fragments in negative cell lines. For siRNA experiments, cells were grown to a confluency of approximately 30% and incubated with 100 μM Dharmacon ON-TARGETplus MUC5AC siRNA (D-001810-02-05; GE Healthcare) or Dharmacon ON-TARGETplus nontargeting siRNA (no. 2, lot 1876332; GE Healthcare) as a control using Dharmacon Dharmafect (GE Healthcare) for 2 d followed by incubation in serum-free medium for another 2 d. The protein samples were analyzed by immune blots with RA96. For expression of recombinant MUC5AC fragments, Cos7 cells and Paca44 cells were transfected with the MUC5AC sequences bearing the pcDNA3.1 expression system as previously described (*12*). N-terminal, C-terminal, and N + 2TR + C-terminal MUC5AC coding sequences and green fluorescent protein–pcDNA3.1 control DNA were transferred to cells using the Effectene transfection procedure (Qiagen). Three days after transfection, the proteins were prepared, separated by NuPAGE 7% gels (Pierce/ThermoFisher Scientific), transferred to an Immobilon-FL (Merck) polyvinylidene fluoride membrane, and probed by RA96 and anti-MUC5AC 2-11M1.

Immunohistochemistry with RA96

The tissue microarray was constructed as described previously (*16*). Briefly, 6 tissue microarrays containing 300 cores of normal ducts and pancreatic intraepithelial neoplasias (PanINs), originating from 21 disease-free pancreata and 81 resected pancreata (because of other neoplasms), 30 alcoholic chronic pancreatitis (CP) and 10 autoimmune pancreatitis specimens, and 48 pancreatic ductal adenocarcinomas (G1–G3) were evaluated. Immunohistochemical staining was performed with RA96, including deparaffinization of the formalin-fixed paraffin-embedded tissue sections and heat-induced antigen retrieval. The intensity of the reactions was scored as mild, moderate, or strong (score 1, 2, or 3, respectively) by an experienced pathologist.

Preparation and Radiolabeling of ^{89}Zr-Desferrioxamine (DFO) Antibodies

RA96 and isotype-matched IgG (~150 kDa) were functionalized with *p*-isothiocyanatobenzyl-DFO (DFO-Bn-NCS; Macrocyclics, Inc.) as described previously (*17*). DFO–antibody conjugates were analyzed via matrix-assisted laser desorption ionization time-of-flight MS and found to have 3–4 chelates per antibody. ^{89}Zr was produced through proton beam bombardment of yttrium foil and isolated in high purity as ^{89}Zr-oxalate at Memorial Sloan Kettering Cancer Center (MSKCC) according to published procedures (*18*). DFO-RA96 and DFO-IgG were incubated with neutralized ^{89}Zr-oxalate in Chelex (Bio-Rad) phosphate-buffered saline at pH 7.0 and 37°C for 1 h. Radioconjugates were purified using disposable size-exclusion (PD-10) columns with phosphate-buffered saline buffer exchange and characterized via instant thin-layer chromatography.

Small-Animal Models

All animal studies were conducted in accordance with the guidelines set by the Institutional Animal Care and Use Committee at MSK. Capan-2 cells (5×10^6/mouse) in 200 μL of 1:1 medium:Matrigel (BD Biosciences) were implanted subcutaneously in the lower right flank of female athymic nude (NU/NU) mice (6–8 wk old and weighing 20–22 g; Charles River Laboratories) and grown to a tumor volume of approximately 100–150 mm^3 (4–5 wk) before imaging studies. Mia PaCa-2, Capan-2, and Capan-1 cells were implanted orthotopically into the head of the pancreas of female athymic nude mice (40,000 cells, 1:1 Matrigel, 20 μL). The tumors were palpated weekly and grown to a volume of approximately 150–200 mm^3 (4–5 wk).

Enzyme-Linked Immunosorbent Assay on Serum Samples

Serum samples were collected from animals 1 wk before imaging studies. MUC5AC levels were detected with a human MUC5AC enzyme-linked immunosorbent assay kit (Aviva Systems Biology) according to the manufacturer's instructions.

In Vivo Imaging

The mice were anesthetized with 1.5%–2% isoflurane (Baxter Healthcare) supplemented with medical air and were injected with ^{89}Zr-DFO-RA96 or ^{89}Zr-DFO-IgG (10–11 MBq, 30–40 μg) in 130–150 μL of phosphate-buffered saline via the lateral tail vein. PET whole-body acquisitions were recorded at 24, 48, 72, 96, 120, and 144 h after injection using a dual small-animal PET/CT scanner (Inveon; Siemens). Images were collected at no less than 50 million coincidence events per animal and reconstructed using standard 2-dimensional ordered-subsets expectation maximization.

Biodistribution Studies

Ex vivo γ-counting of tissues was performed to measure the uptake of the radioconjugate in tissues at 144 h after radiotracer administration. Radioactivity within each organ was counted using a PerkinElmer γ-counter with isotope-dependent calibrated protocols. Tracer uptake expressed as percentage injected dose per gram (%ID/g) was calculated as the radioactivity associated with each tissue divided by the organ mass, using the mass of the decay-corrected injected dose at the time of counting.

Statistical Considerations

All data were analyzed by the unpaired, 2-tailed Student *t* test, and differences at the 95% confidence level ($P < 0.05$) were considered statistically significant. Positive and negative controls were included whenever possible to ensure rigor and reproducibility throughout the experimental design.

RESULTS

MS Analysis Identifies MUC5AC Target

To characterize the Ra96 antigen, we performed secretome analyses. By immune detection of secretomes and lysates of the cell lines and by immune fluorescence analyses of PC cell lines, we selected the RA96-reactive and nonreactive cells. The cell line Capan-1 secreted the highest amounts of RA96 antigen, followed by A818, BxPC3, and Panc1. MiaPaCa2, Panctu II, Paca44, and the human pancreatic duct epithelial cells show no detectable reactivity for RA96 antibodies (Supplemental Fig. 1). The RA96 antigen is a high-molecular-weight protein that is sensitive against reducing conditions and disappeared after treatment of the samples with dithiothreitol. For MS analysis, we chose Panctu II as the negative cells and A818 cells as the positive cells because of the more focused region in Western blots than for Capan-1. MS results were compiled in an additional file (Supplemental Fig. 2). Only MUC5AC was exclusively found with maximally 5 unique peptides in the secretome samples from RA96-reactive cell lines with or without immunoprecipitation (the supplemental materials include tables of the MS results).

Immunoprecipitation Confirms MUC5AC at RA96 Target

To confirm the conclusion of the MS results, we performed immunoprecipitation with RA96 and in parallel with MUC5AC monoclonal antibody 2-11M1 (Biomol) in the same experiments (Supplemental Fig. 3) and tested the immune complexes with the antibodies and vice versa. The immune-precipitated proteins isolated by 2-11M1 antibodies were recognized by RA96 antibodies, and the proteins immune-precipitated by RA96 were also recognized by anti MUC5AC clone 2-11M1. A MUC5AC N-terminal peptide (Sigma-Aldrich) was used for competition of the RA96 immune signals in Western blots. The signal intensity of the 2-11M1 antibody could be reduced to 50% by treatment with a 10 μg/mL concentration of N-terminal peptide, whereas this treatment was not sufficient to significantly diminish the RA96 signals (data not shown).

MUC5AC siRNA Experiments and Reexpression Confirms RA96 Specificity

We used siRNA on-target, as well as for knockdown of Muc5AC expression in positive cells (Supplemental Figs. 4A and 4B). In Western blots, the RA96 signal intensity dropped to 20% of the untreated sample. To characterize the epitope of RA96 in more detail, we performed MUC5AC reexpression experiments. The constructs were described by Ryan et al. (kindly provided to us by Marguerite Clyne and Colm Reid), and coding for MUC5AC (N-terminal, C-terminal, and N + 2TR + C-terminal fragments) was used in Cos7 control cells (*12*). RA96 and anti-MUC5AC 2-11M1 recognized the lysates of MUC5AC-transfected cells with the N + 2TR + C-terminal construct and with the N-terminal (Supplementary Fig. 4C). Neither RA96 nor 2-11M1 detected the C-terminal fragment. The expression of the C-terminal part in transfected Cos7 cells was checked with the help of the flag tags on the C-terminal construct (data not shown).

Immunohistochemistry with RA96 Highlights Specificity for PC Lesions over CP

RA96 shows positive staining and a specific progression of severity in clinical samples. Positive staining begins at the PanIN level and increases in different grades of pancreatic ductal adenocarcinoma, including staining in capan-2 xenografts (Fig. 1). There is little to no staining in the CP samples, highlighting specificity for PC over other inflammatory conditions that are often conflated by serum biomarkers. Clinical immunohistochemistry is tabulated and quantified in Supplemental Figure 5 (*19*).

^{89}Zr-DFO-RA96 Shows Significant Tumor Delineation in Capan-2 Xenografts

Multiple stoichiometric ratios (×10, ×20, and ×40) of chelator (DFO) to antibody (RA96 or IgG) were characterized via matrix-

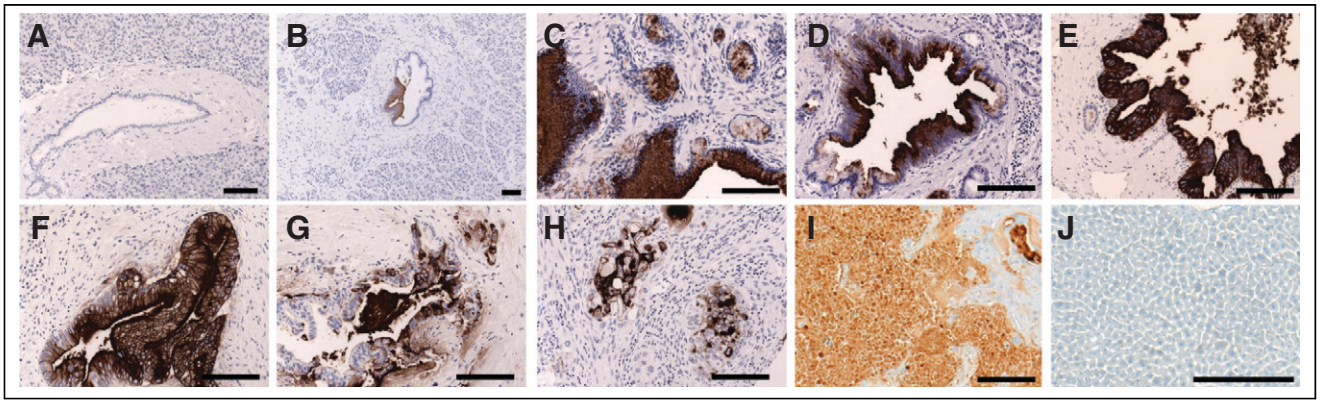

FIGURE 1. Immunohistochemistry of MUC5AC with RA96. (A) No expression of RA96 in normal human pancreas. (B) No or weak expression in chronic pancreatitis. (C–E) Strong staining with RA96 in PanINs 1–3. (F–H) Moderate to strong expression in pancreatic ductal adenocarcinoma of different grades. More detail is provided in supplemental materials with regard to grade and scoring. (I) Capan-2 xenografts also staining positively with RA96. (J) Control tissue showing no background staining in liver. Each line indicates 50 μm.

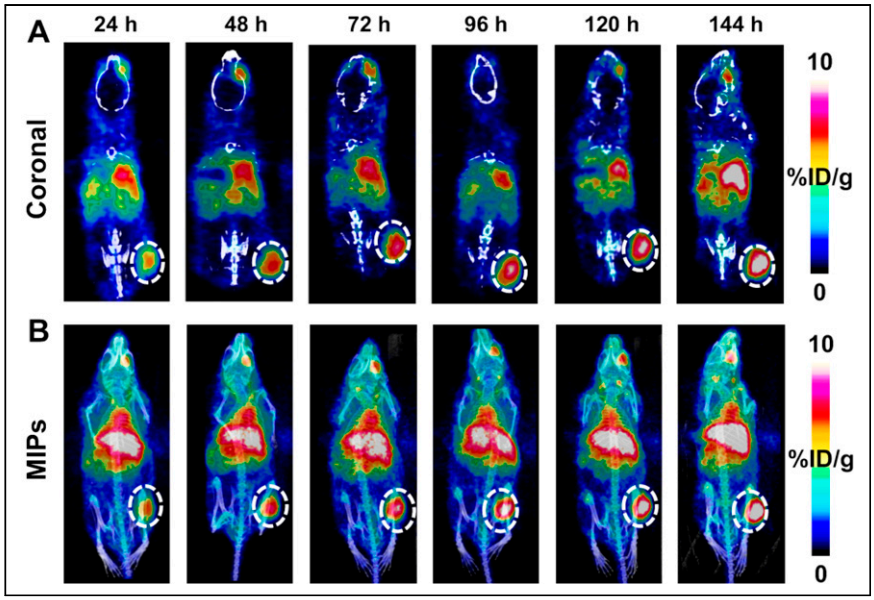

FIGURE 2. Serial PET/CT imaging of ^{89}Zr-DFO-RA96 over course of 144 h. Images are represented as coronal slices (A) and maximum-intensity projections (MIPs) (B). Tumors are on right flank and encircled by dotted line. Mice were retroorbitally bled from right eye 1 wk previously, resulting in nonspecific uptake of radiotracer in eye region. Increasing uptake of radiotracer in tumor is shown over time, with maximum at 144 h.

assisted light desorption ionization time-of-flight MS. Reaction conditions that resulted in DFO-RA96 and DFO-IgG with an average of 3–4 chelators per antibody were used in further radiolabeling procedures. All radiotracers were examined for their stability in serum; each showed more than 95% stability out to 1 wk for RA96 and more than 90% stability for IgG radiolabeled constructs (Supplemental Fig. 6). The radiochemical yield for each reaction ranged from 90% to 95%, and all tracers used in vivo were processed to a radiochemical purity of more than 99%. The specific activity and molar activity for both ^{89}Zr-DFO-RA96 and ^{89}Zr-DFO-IgG were 0.3–0.4 MBq/μg and 45–55 GBq/μmol, respectively. Serial PET imaging with ^{89}Zr-DFO-RA96 shows significant uptake (14.6 ± 1.5 %ID/g) compared with the blocking group (6.6 ± 1.5 %ID/g) and ^{89}Zr-DFO-IgG (8.8 ± 0.3 %ID/g), with a P value of less than 0.001 for both. In capan-2 tumors, increased accumulation of antibody was observed over the course of 144 h (Fig. 2), as expected for antibody-based radiotracers. To mitigate liver uptake for a shed serum biomarker, we tried the preinjection strategy as previously described by Houghton et al. with anti-CA19-9 radiotracer (*20*). To mimic these studies, we preinjected a ×3 cold dose (unlabeled RA96) 4 h before ^{89}Zr-DFO-RA96 administration. Interestingly, we observed a partial block of the system, with no statistical difference between ^{89}Zr-DFO-RA96 tumor uptake via a ×3 preinjection or a ×30 cold blocking dose coinjection (6.2 ± 0.8 %ID/g for the ×3 preinjection vs. 6.6 ± 1.5 %ID/g for the ×30 coinjection). The ×30 dose was specifically administered for blocking purposes to confirm the specificity of the RA96 tracer. The block and partial-block groups, along with the ^{89}Zr-DFO-IgG arm, have a P value of less than 0.001 when compared with the specific uptake of ^{89}Zr-DFO-RA96 in the tumor (Fig. 3). This can also be observed as early as 24 h and is consistent at 72 h as well (Supplemental Figs. 7 and 8). We performed an enzyme-linked immunosorbent assay experiment on serum samples collected from capan-2 mice 1 wk before PET imaging experiments to assess the degree of MUC5AC antigen shedding in this model. We could not find any detectable MUC5AC in serum samples of these animals, despite the successful calibration curve and quality controls for the kit (Supplemental Fig. 9). These results are consistent with our partial block of our target from the preinjection of unlabeled antibody.

^{89}Zr-DFO-RA96 Shows Significant Tumor Delineation in Orthotopic Xenografts of Varying MUC5AC Expression

To further expand on the utility of this tracer, we inoculated animals orthotopically with tumors of varying MUC5AC expression and RA96 immunogenicity. We found that the uptake did indeed correlate with low, medium, and high MUC5AC expression in orthotopic models of MIA PaCA-2, Capan-2, and Capan-1, respectively (Fig. 4). Additional imaging of this cohort at 72 h can be found in Supplemental Figure 10.

DISCUSSION

With all these data taken together, we were able to confirm that RA96 can demarcate MUC5AC expression in PC tumors. Our immuno-PET tracer ^{89}Zr-DFO-RA96 shows excellent and specific tumor delineation in MUC5AC-positive tumors that can be blocked with both a partial and excess administration of unlabeled RA96. Although the capan-2 tumor model has been characterized as a shed antigen model for serum biomarker CA19-9 (*20*), we did not observe significant shedding of MUC5AC, despite clinical data showing a similar effect of this secreted biomarker (*9*). Moreover, we also indicate that ^{89}Zr-DFO-RA96 is able to detect orthotopic lesions in multiple models of PC of varying MUC5AC expression. Finally, RA96 is multipurposed in its ability to serve as an antibody for immunohistochemistry, successfully delineating CP from PC through staining of MUC5AC in PanINs and increasing grades of pancreatic ductal adenocarcinoma. We show strong evidence that this biomarker, antibody, and radiotracer have great potential for the field of PC diagnostics through multiple modalities.

Repeat biopsies are invasive and often lack reproducibility because of sampling issues, particularly in heterogeneous tumors such as PC. More importantly, biopsies may not be particularly useful for patients with widespread metastasis, which is often the case for PC. A whole-body imaging agent that is specific for PC over CP could serve as an early diagnostic for PanINs and would be a game-changing biomarker that serves to fulfill a diagnostic niche that the field of PC is desperately missing. Currently, the standard for diagnostic imaging of PC in the clinic is typically CT or MRI. Although these techniques can be sufficient for diagnostic purposes, CT and MRI do not offer all the advantages that PET does in terms of quantitative measurement of a specific biomarker.

Establishing biomarkers in PC is a critically unmet need to improve the prognosis of this challenging disease. Although several diagnostic biomarkers for PC have been investigated, most have yielded suboptimal results (*21–23*). CA19-9, a blood-based biomarker for follow-up, is useful for disease prognosis but has limited utility as an early detection marker due to its variable sensitivity (60%–90%), specificity (68%–91%), and positive predictive value (0.9%–2.4%) (*24,25*). Additionally, CA19-9 can be elevated

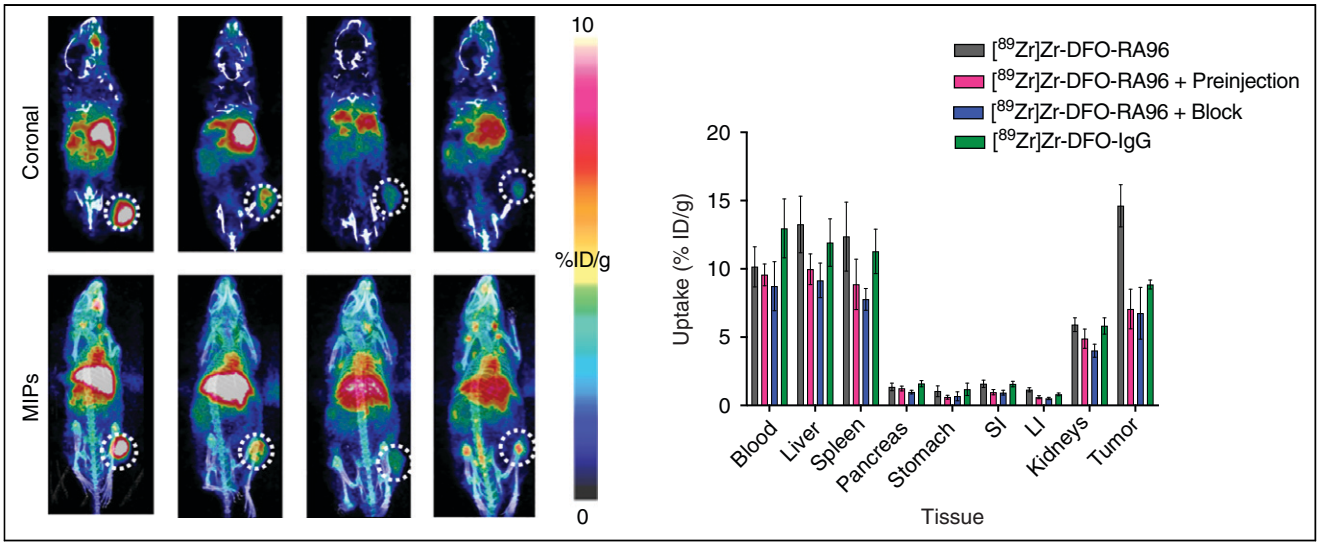

FIGURE 3. Serial PET/CT imaging of ^{89}Zr-DFO-RA96 and ^{89}Zr-DFO-IgG, with corresponding ex vivo biodistribution at 144 h. Images are represented as coronal slices (A) and maximum-intensity projections (MIPs) (B). Tumors are on right flank and encircled by dotted line. Significant differences are noted when comparing ^{89}Zr-DFO-RA96 with all control groups ($P < 0.001$). "Preinjection" indicates partial block, with ×3 amount of unlabeled antibody injected 4 h before injection with ^{89}Zr-DFO-RA96. "Block" indicates full block with ×30 amount of unlabeled antibody coinjected with ^{89}Zr-DFO-RA96. "IgG" indicates injection of isotype-matched control ^{89}Zr-DFO-IgG. Mice were retroorbitally bled from right eye 1 wk previously, resulting in nonspecific uptake of radiotracer in eye region. LI = large intestine; SI = small intestine.

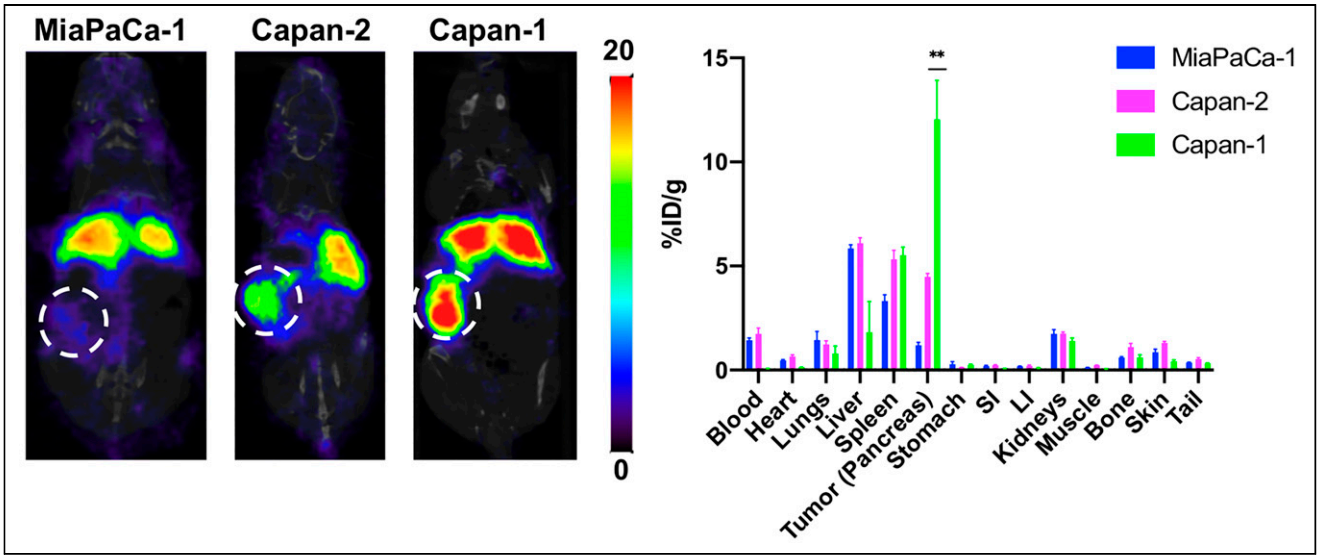

FIGURE 4. PET/CT imaging of ^{89}Zr-DFO-RA96, with corresponding ex vivo biodistribution at 144 h in multiple orthotopic tumor models. Images are represented as coronal slices, and tumors are encircled by dotted line. From left to right: MiaPaCa-1 tumors (low MUC5AC expression), Capan-2 tumors (medium MUC5AC expression), and Capan-1 tumors (high MUC5AC expression). LI = large intestine; SI = small intestine.

in benign conditions such as CP, jaundice, and cirrhosis. Furthermore, approximately 5%–10% of Caucasians are unable to synthesize CA19-9 (*25–27*), which makes it challenging for widespread reliability as a biomarker in the clinic. Approximately 65% of resectable PC cases have elevated levels of CA19-9 in the blood (*21*). In light of the sporadic nature of PC and asymptomatic early disease stages, identification and characterization of serum markers that can either complement or outperform CA19-9 are highly desirable.

Previous studies have shown that CA19-9 levels can predict stage and survival in resectable PC (*28*) and in locally unresectable PC (*29*). Multiple recent studies have also revealed the nonspecific nature of CA19-9 as a diagnostic marker (*2–4,30*). Several promising studies focus on CA19-9 for both imaging and radioimmunotherapy (*31,32*) and are ongoing at MSK. We aim to apply our expertise in order to evaluate novel biomarkers for both early and specific detection of PC and to drive the improvement of clinical outcomes for this devastating disease. Clinical gold standard

metabolic radiotracers such as ^{18}F-FDG are often nonspecific for malignancy (*33*). Our MUC5AC-targeted radiotracer could fill the gap that exists for serum biomarkers and serve to fulfill an unmet need for early diagnosis in PC.

CONCLUSION

Current biomarkers for PC are unreliable when it comes to differentiating between inflammation and malignancy. The RA96 antibody has been well characterized to be a MUC5AC conformation–dependent antigen. RA96 has the ability to achieve early detection of PC as it can detect lesions from PanINs all the way to fully developed pancreatic ductal adenocarcinoma via immunohistochemistry, as well as specifically demarcate PC from CP in patient samples. We have successfully developed an immuno-PET tracer with RA96 and shown that it can noninvasively and specifically demarcate MUC5AC expression in PC. We expect that immuno-PET targeting MUC5AC has high potential to be clinically useful for early detection of PC.

DISCLOSURE

Assistance was received from the Antibody & Bioresource, Small Animal Imaging, and Radiochemistry and Molecular Imaging Probe Core Facilities at MSK, which are supported in part by NIH grant P30 CA08748. Financial support was received from Mr. William H. Goodwin and Mrs. Alice Goodwin and the Commonwealth Foundation for Cancer Research and the Experimental Therapeutics Center of MSK (Jan Grimm) and from NIH grant R35 CA232130-01A1 (Jason Lewis) and the MSK Center for Molecular Imaging and Nanotechnology Tow Fellowship (Kelly Henry). A part of this study was funded by P.U.R.E. (Protein Research Unit Ruhr within Europe), Ministry of Innovation, Science, and Research of North-Rhine Westphalia, Germany. Jan Grimm and Jason S. Lewis are both associate editors of *The Journal of Nuclear Medicine*. No other potential conflict of interest relevant to this article was reported.

ACKNOWLEDGMENTS

We acknowledge BioRender for preparing the graphical abstract. This work is dedicated to the late Prof. Siegfried Matzku, DKFZ, Heidelberg, Germany, who initiated in vivo targeting strategies decades ago. We also sincerely appreciate the long-standing support of Prof. Günter Klöppel, now Pathology Munich, who helped to select the best candidates from an overwhelming number of hybridoma cultures during the common projects in Hamburg.

KEY POINTS

QUESTION: The central hypothesis of this study is that our MUC5AC-targeted antibody RA96 could detect PC lesions that are specific from other instances of inflammation such as CP.

PERTINENT FINDINGS: We demonstrate that our immuno-PET strategy can be used to noninvasively detect MUC5AC expression in PC, a key serum biomarker that is able to not only detect PanINs but also specifically demarcate PC from CP.

IMPLICATIONS FOR PATIENT CARE: There is a critical need for developing better biomarkers to improve early detection of PC. Current biomarkers for PC are unreliable when it comes to differentiating between inflammation and malignancy. ^{89}Zr-DFO-RA96 could be a valuable tool to specifically demarcate PC from CP and detect early-onset PanINs.

REFERENCES

1. McGuigan A, Kelly P, Turkington RC, Jones C, Coleman HG, McCain RS. Pancreatic cancer: a review of clinical diagnosis, epidemiology, treatment and outcomes. *World J Gastroenterol.* 2018;24:4846–4861.
2. Song J, Sokoll LJ, Pasay JJ, et al. Identification of serum biomarker panels for the early detection of pancreatic cancer. *Cancer Epidemiol Biomarkers Prev.* 2019;28:174–182.
3. Ballehaninna UK, Chamberlain RS. Serum CA 19-9 as a biomarker for pancreatic cancer: a comprehensive review. *Indian J Surg Oncol.* 2011;2:88–100.
4. Ballehaninna UK, Chamberlain RS. The clinical utility of serum CA 19-9 in the diagnosis, prognosis and management of pancreatic adenocarcinoma: an evidence based appraisal. *J Gastrointest Oncol.* 2012;3:105–119.
5. Kato S, Hokari R, Crawley S, et al. MUC5AC mucin gene regulation in pancreatic cancer cells. *Int J Oncol.* 2006;29:33–40.
6. Rachagani S, Torres MP, Kumar S, et al. Mucin (Muc) expression during pancreatic cancer progression in spontaneous mouse model: potential implications for diagnosis and therapy. *J Hematol Oncol.* 2012;5:68.
7. Iacobuzio-Donahue CA, Velculescu VE, Wolfgang CL, Hruban RH. Genetic basis of pancreas cancer development and progression: insights from whole-exome and whole-genome sequencing. *Clin Cancer Res.* 2012;18:4257–4265.
8. Matull WR, Andreola F, Loh A, et al. MUC4 and MUC5AC are highly specific tumour-associated mucins in biliary tract cancer. *Br J Cancer.* 2008;98:1675–1681.
9. Kaur S, Smith LM, Patel A, et al. A Combination of MUC5AC and CA19-9 improves the diagnosis of pancreatic cancer: a multicenter study. *Am J Gastroenterol.* 2017;112:172–183.
10. Kim GE, Bae HI, Park HU, et al. Aberrant expression of MUC5AC and MUC6 gastric mucins and sialyl Tn antigen in intraepithelial neoplasms of the pancreas. *Gastroenterology.* 2002;123:1052–1060.
11. Adamczyk KA, Klein-Scory S, Tehrani MM, et al. Characterization of soluble and exosomal forms of the EGFR released from pancreatic cancer cells. *Life Sci.* 2011;89:304–312.
12. Ryan A, Smith A, Moore P, et al. Expression and characterization of a novel recombinant version of the secreted human mucin MUC5AC in airway cell lines. *Biochemistry.* 2015;54:1089–1099.
13. Nollet S, Escande F, Buisine MP, et al. Mapping of SOMU1 and M1 epitopes on the apomucin encoded by the 5′ end of the MUC5AC gene. *Hybrid Hybridomics.* 2004;23:93–99.
14. Witzke KE, Rosowski K, Müller C, et al. Quantitative secretome analysis of activated Jurkat cells using click chemistry-based enrichment of secreted glycoproteins. *J Proteome Res.* 2017;16:137–146.
15. Kalthoff H, Schmiegel W-H, Auerswald U, et al. Monoclonal antibody RA-96 defines a new mucin antigen in pancreatic cancer. *Digestion.* 1988;40:90.
16. Neesse A, Hahnenkamp A, Griesmann H, et al. Claudin-4-targeted optical imaging detects pancreatic cancer and its precursor lesions. *Gut.* 2013;62:1034–1043.
17. Henry KE, Dacek MM, Dilling TR, et al. A PET imaging strategy for interrogating target engagement and oncogene status in pancreatic cancer. *Clin Cancer Res.* 2019;25:166–176.
18. Holland JP, Sheh Y, Lewis JS. Standardized methods for the production of high specific-activity zirconium-89. *Nucl Med Biol.* 2009;36:729–739.
19. Juhl H, Stritzel M, Wroblewski A, et al. Immunocytological detection of micrometastatic cells: comparative evaluation of findings in the peritoneal cavity and the bone marrow of gastric, colorectal and pancreatic cancer patients. *Int J Cancer.* 1994;57:330–335.
20. Houghton JL, Abdel-Atti D, Scholz WW, Lewis JS. Preloading with unlabeled CA19.9 targeted human monoclonal antibody leads to improved PET imaging with ^{89}Zr-5B1. *Mol Pharm.* 2017;14:908–915.
21. Goggins M. Molecular markers of early pancreatic cancer. *J Clin Oncol.* 2005;23:4524–4531.
22. Kaur S, Baine MJ, Jain M, Sasson AR, Batra SK. Early diagnosis of pancreatic cancer: challenges and new developments. *Biomark Med.* 2012;6:597–612.
23. Koopmann J, Rosenzweig CNW, Zhang Z, et al. Serum markers in patients with resectable pancreatic adenocarcinoma: macrophage inhibitory cytokine 1 versus CA19-9. *Clin Cancer Res.* 2006;12:442–446.
24. Locker GY, Hamilton S, Harris J, et al. ASCO 2006 update of recommendations for the use of tumor markers in gastrointestinal cancer. *J Clin Oncol.* 2006;24:5313–5327.
25. Duffy MJ, Sturgeon C, Lamerz R, et al. Tumor markers in pancreatic cancer: a European Group on Tumor Markers (EGTM) status report. *Ann Oncol.* 2010;21:441–447.
26. Brody JR, Witkiewicz AK, Yeo CJ. The past, present, and future of biomarkers: a need for molecular beacons for the clinical management of pancreatic cancer. *Adv Surg.* 2011;45:301–321.
27. Ghaneh P, Costello E, Neoptolemos JP. Biology and management of pancreatic cancer. *Postgrad Med J.* 2008;84:478–497.

28. Ferrone CR, Finkelstein DM, Thayer SP, Muzikansky A, Fernandez-delCastillo C, Warshaw AL. Perioperative CA19-9 levels can predict stage and survival in patients with resectable pancreatic adenocarcinoma. *J Clin Oncol.* 2006;24:2897–2902.
29. Yang GY, Malik NK, Chandrasekhar R, et al. Change in CA 19-9 levels after chemoradiotherapy predicts survival in patients with locally advanced unresectable pancreatic cancer. *J Gastrointest Oncol.* 2013;4:361–369.
30. Wong S-J, Hong C-M, Wang H-P, Cheng T-Y. High serum level of CA 19-9 not always related to the pancreas: an asymptomatic case of highly elevated CA 19-9 related to lung adenocarcinoma. *J Pancreas.* 2016;17:653–655.
31. Lohrmann C, O'Reilly EM, O'Donoghue JA, et al. Retooling a blood-based biomarker: phase I assessment of the high-affinity CA19-9 antibody HuMab-5B1 for immuno-PET imaging of pancreatic cancer. *Clin Cancer Res.* 2019;25:7014–7023.
32. Poty S, Carter LM, Mandleywala K, et al. Leveraging bioorthogonal click chemistry to improve ^{225}Ac-radioimmunotherapy of pancreatic ductal adenocarcinoma. *Clin Cancer Res.* 2019;25:868–880.
33. Ibrahim N, Cho S, Hall L, Perlman S. Is it cancer? Potential pitfalls of FDG PET/CT imaging [abstract]. *J Nucl Med.* 2016;57(suppl 2):1315.